ACS APPLIED MATERIALS & INTERFACES

Forum Article

www.acsami.org

Programmable Mechanically Assisted Geometric Deformations of Glassy Two-Stage Reactive Polymeric Materials

Maciej Podgórski,[†,‡] Devatha P. Nair,[†] Shunsuke Chatani,[†] Gayla Berg,[†] and Christopher N. Bowman*[,†]

[†]Department of Chemical and Biological Engineering, University of Colorado, UCB 596, Boulder, Colorado 80309, United States

[‡]Faculty of Chemistry, Department of Polymer Chemistry, MCS University, pl. Marii Curie-Skłodowskiej 5, 20-031 Lublin, Poland

Supporting Information

ABSTRACT: Thiol-isocyanate-methacrylate two-stage reactive network polymers were developed and used for fabrication of well-defined surface patterns as well as functional geometric shapes to demonstrate a new methodology for processing of "smart materials". The dynamic stage I networks were synthesized in base-catalyzed thiol-isocyanate cross-linking reactions to yield tough, glassy materials at ambient conditions. Methacrylate-rich stage I networks, incorporating photoinitiator and photoabsorber, were irradiated with UV light to generate stage II networks with intricate property gradients. Upon directional straining and subsequent temperature-dependent stress relief of the predefined gradient regions, the desired surface or bulk geometric transformations were achieved. Depending on the gradient extent in conjunction with photoorthogonal initiators, the introduced deformations were shown to be easily erasable by heat or permanently fixable by bulk polymerization.

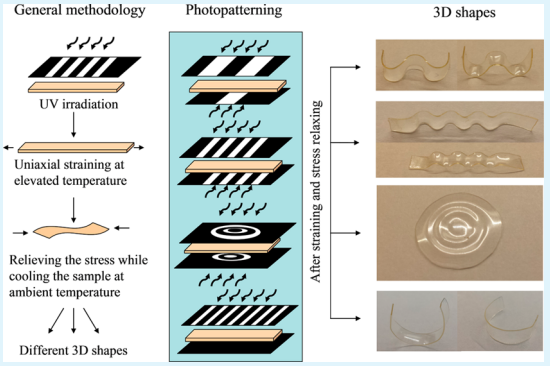

KEYWORDS: *stimuli-responsive materials, photopatterning, shape memory, thiol-Michael addition, thiol isocyanate reaction*

INTRODUCTION

The capability of dynamic or actively moving polymeric materials, which upon the application of an external stimulus can change their shape and/or surface features in a predefined way, has attracted tremendous attention in many research areas. Because of their extraordinary capabilities, smart materials have been exploited in applications spanning disciplines like microfluidics, electronics, optics and biomedicine to name a few.[1−7] Three-dimensional shape change associated with shape-memory polymers (SMPs) is one distinct and exciting example of a broad class of smart materials that find applications in fabrication of biomedical devices[8,9] among other applications.

Depending on the target application, SMPs are frequently prepared from loosely cross-linked poly(ethylene glycol)[10] (PEG), poly(vinyl alcohol)[11] (PVA), or poly(3-caprolactone)[12] (PCL), often modified by the addition of reinforcing fillers such as carbon nanotubes and silica nanoparticles.[13,14] Regardless of the application, the shape memory effect (SME) in an overwhelming magnitude of examples is based on the one-way transition from a temporary "programmed" shape to a permanent final shape. Various stimuli such as heat, light, moisture, electricity or magnetism have been used to induce the shape transition.[15−17]

On the other hand, externally triggered/imposed topographic changes on polymeric surfaces, which represent another class of stimuli-responsive materials, have found numerous applications in antifouling coatings[18,19] adhesives,[20] or microarray lenses.[1,21] Varying in scale and nature of the deformation, the chemistries involved in fabrication of SMPs that result in distinct surface topographies can also vary extensively. Current strategies for creating desired surface morphologies involve a wrinkling phenomenon by buckling a bilayer system in which a thin hard film resides on top of a soft expanded substrate, such as explored in poly(dimethylsiloxane) (PDMS).[22,23] The surface patterns are achieved by consecutively straining the PDMS foundation layer, depositing or forming a skin layer, and then releasing the deformation of the foundation. This last step exerts a lateral compressive force on the skin layer, thereby causing it to buckle. The controlled deformation of PDMS can also be induced via thermal expansion or by swelling in organic solvents.[4,23,24] In general, the manipulation of pattern transition and its evolution within a polymer can be tuned by a variety of factors including the extent of mechanical instability imposed (strain), modulus difference between the layers, the direction of the applied strain, and the film thickness among others.

Beside this approach, new chemistries are continuously being developed and probed for fabrication of well-defined topographical features or textures. One interesting example describes mechanophotopatterning of a photoresponsive elastomeric material that allows for precise as well as simultaneous manipulation of both material shape and surface

Special Issue: Applications of Hierarchical Polymer Materials from Nano to Macro

Received: November 25, 2013
Accepted: January 2, 2014
Published: January 10, 2014

   dx.doi.org/10.1021/am405371r | *ACS Appl. Mater. Interfaces* 2014, 6, 6111−6119

topography.[25] The inclusion of AFCT-capable (addition−fragmentation chain transfer) functionalities, either in the network backbone or at linkage points within the network, enabled network rearrangement upon radical photogeneration. This approach provides a means for the generation of distinct and robust topologies on material surfaces with exquisite spatial and temporal control.

Recently, a dual cure approach in creating a polymer network system was proposed for a range of material applications, including SMPs, impression materials, and refractive index structures.[9,26] This two-stage polymerization strategy employed two orthogonal reactions, namely, a thiol-Michael addition reaction and a free radical polymerization within the same polymer network to generate a matrix with distinct properties at the end of each stage. By designing an off-stoichiometric thiol-vinyl polymer network with excess vinyl functionality, an initial cross-linked polymer network was generated via the thiol-Michael reaction. As an outcome, the stage I network was a loosely cross-linked, low modulus polymer with idealized properties that enabled further processing such as molding and reshaping to generate intricate topographical imprints. Once processing was complete, the network was further cross-linked via a radical-initiated vinyl homopolymerization to permanently hold its new shape. In recent ground breaking work, Kloxin and coworkers utilized a similar strategy in a different way to buckle the surface of a thiol−acrylate elastomer by introducing a cross-linking gradient within the film.[27] In this methodology, the second photopolymerization stage was carried out on strained samples containing a UV absorber that confined the UV light-induced cross-linking of the excess monomer primarily to the upper layers, which in turn facilitated wrinkle formation upon bulk release of the strain. The authors also showed photo-orthogonality in systems containing photoorthogonal initiators by demonstrating that the bulk polymer can be easily molded into the desired geometries after the wrinkling process is complete.

To-date, the majority of the research in this area has dealt with soft matter, i.e., materials that are rubbery at ambient temperatures and/or with low cross-linking densities that rarely exceed 20 MPa.[3] This approach is not without justification as the material processing involved in creating surface features, be it via a chemical reaction or the physical reshaping induced via photopatterning or molding is far more efficient in loosely cross-linked, soft materials with a high degree of molecular mobility. On the other hand, low glass-transition temperatures and the lack of toughness of these materials preclude them from several applications that require hard and glassy materials with long durability at ambient conditions.

Inspired by the previous work, here we employ a modified two-stage polymerization strategy where ambient temperature glassy networks are formed after both polymerization stages. By implementing the thiol-isocyanate cross-linking reaction to form the initial polymer network, uniform and tough thiourethane networks are developed with glass transition temperatures in the range 40−70 °C. The initial stage I networks were designed to contain a fixed amount of fully tethered methacrylate functionalities that served as reactive sites for stage II methacrylate homopolymerization. The extent of cure, modulus development and materials processability was evaluated in stage II networks with varied content of pendant double bonds versus stage I cross-linking densities. Further, the use of UV absorber and photo-orthogonal initiators enabled stage I network mechanoprogramming into desired 3D structures that could be either temperature-erased or fixed on demand. Predefined surface topographies were shown to be easily achievable and tunable with the possibility of permanent fixing. The reported two-stage methodology when combined with a mechanophotopatterning technique results in materials that can posses two structurally different working geometries both of which are tough networks with T_g values well above ambient.

EXPERIMENTAL SECTION

Materials. Pentaerythritol tetrakis(3-mercaptopropionate) (PETMP) was donated by Bruno Bock. Triphenylphosphine (TPP), methanesulfonic acid (MsOH), hexamethylene diisocyanate (HMDI), 2-isocyanatoethyl methacrylate (IEM), thioacetic acid (TA), 1,3,5-triallyl-1,3,5-triazine-2,4,6(1H,3H,5H)-trione (TATATO), 2,2-azobis-(2-methylpropionitrile) (AIBN), and *d*-chloroform were purchased from Sigma-Aldrich. Divinyl sulfone (DVS) was purchased from Oakwood Chemicals. Irgacure 651 (2,2-dimethoxy-2-phenylacetophenone−DMPA), Irgacure 819 (Bis(2,4,6-trimethylbenzoyl)-phenylphosphineoxide−BPO), and Tinuvin 328 (T328) (2-(2H-benzotriazol-2-yl)-4,6-ditertpentylphenol) were obtained from BASF. AIBN was recrystallized from methanol before use. Other chemicals were used without purification.

Synthesis of 1,3,5-Tris(3-mercaptopropyl)-1,3,5-triazine-2,4,6-trione (TTT-SH). The aliphatic TATATO-derived trithiol was synthesized according to the two-step procedure described by Lundberg et al.[28] In short, 1,3,5-triallyl-1,3,5-triazine-2,4,6-(1H,3H,5H)-trione (TATATO) and thioacetic acid (TA) in 10 wt % excess were reacted through a radical thiol−ene reaction carried out in the presence of 2,2-azobis(2-methylpropionitrile) (AIBN) (1 wt %) at 65 °C for 6 h. In the second step hydrolytic cleavage of the thioester was performed overnight at 60 °C in methanol and concentrated hydrochloric acid, both used at a volumetric ratio of 2/1. After purification, a yellowish viscous liquid was obtained (yield: 65−70 %). Monomer identification data can be found in the Supporting Information.

Network Fabrication. All PETMP-containing samples incorporated TPP/DVS/MsOH as an initiating system at a fixed component ratio of 1.5/3/0.2 wt %. The TTT-SH samples contained TPP/DVS at the wt % ratio of 1/1. TPP and MsOH were added to the thiol and mixed thoroughly. HMDI, IEM, DVS, IR 651 (1 wt %) and optionally IR 819 (1 wt %), and/or T328 (0.6 wt %) were mixed vigorously in a separate vial. The isocyanates were then added to the thiols and paddle-mixed until homogenous mixtures were obtained. Three PETMP/HMDI/IEM formulations were prepared at the molar (M) ratios of 2M/3.33M/1.33M, 2M/3M/2M, and 2M/2.66M/2.66M, respectively. Also, TTT-SH/HMDI/IEM system at a 1/1/1 molar ratio was prepared. The first-stage films were cured at 365 nm light with either 5 or 50 mW/cm^2 light intensity depending on the experiment type.

Fourier Transform Infrared Spectroscopy (FT-IR). FT-IR experiments were performed on a Nicolet Magna 760 spectrometer. The methacrylate photopolymerization conversion vs. time plot was obtained by measuring the decrease in the intensity of the double bond peak absorbance at 6160 cm^{-1}. A UV 365 nm light source with 50 mW/cm^2 light intensity was directed to the sample through a liquid light guide equipped with a collimating lens and notch filter (365 nm). The thiol-isocyanate reaction conversion was assessed by measuring the increase in the intensity of the thiourethane signal at 6620 cm^{-1}. Experiments were performed on neat 0.25 mm thick stage I films (near-IR) under ambient conditions. Conversions were calculated using the ratio of peak areas to the peak area prior to the reaction.

^{1}H NMR Spectroscopy. NMR spectra were recorded on a Bruker Avance-III 400 NMR spectrometer at 25 °C in d-chloroform. Chemical shifts are reported in parts per million (ppm) relative to tetramethylsilane (TMS).

Dynamic Mechanical Analysis (DMA). DMA experiments were performed using a TA Instruments Q800 dynamic mechanical analyzer. Sample dimensions were 10 × 4 × 1 mm (no T328) or 10

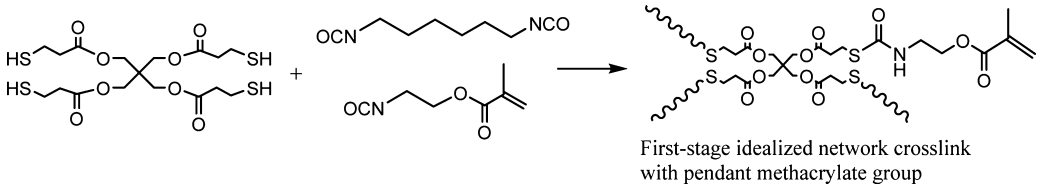

Figure 1. Schematic of first-stage thiol-isocyanate step-growth cross-linking reaction for the PETMP/HMDI/IEM system with 2.0 M thiol, 3.0 M diisocyanate, and 2.0 M 2-isocyanoethyl methacrylate. The initiator system was composed of 1.5 wt.% TPP, 0.2 wt.% MsOH, and 3 wt.% DVS.

× 4 × 0.25 mm (with T328). Sample temperature was ramped at 3 °C/min with a frequency of 1 Hz and a strain of 0.01 %. Glass-transition temperature (T_g) was assigned as the temperature at the peak of the tan δ curve. The rubbery modulus was measured at T_g + 30 °C.

Mechanophotopatterning and Profilometry. If used, the mask was mounted over the unstretched sample and irradiated with the light from UV lamp (Black-Ray Model B100AP). The intensity at the location of the sample was measured using a radiometer equipped with a GaAsP detector. The apparatus used to uniaxially stretch the samples was build of a simple manually controlled micrometer linear stages fixed on an optical platform. Surface topography of the patterned samples was determined using stylus profilometry (Dektak 200VSi stylus profilometer—Veeco). Three photomasks with 5, 10, and 100 μm strips separated by 500 or 150 μm screening gaps were used.

RESULTS AND DISCUSSION

Stage I/Stage II Thiourethane-Methacrylate Network Synthesis and Characterization. Thiol-isocyanate-methacrylate glassy network polymers were formulated via an initial polymerization reaction that was catalyzed by a multicomponent base-generating system composed of a nucleophile, an electron deficient vinyl and an acid. Recent work by Chatani et al. has shown that the onset of the base catalyzed thiol-isocyanate reaction can be delayed when a weak nucleophile such as triphenylphosphine is used as a co-catalyst with a Michael acceptor such as an acrylate or vinyl sulfone, along with catalytic quantities of an acid.[29] Employing the 3-part initiating system enables the advantages of both predictable induction times along with high monomer conversions and rapid kinetics that subsequently follow the induction times. The 3-part initiating system allows for facile processing and molding of otherwise instantaneously reacting mixtures. Consequently, for preparing PETMP/HMDI/IEM formulations, a mixture of a TPP/DVS/MsOH initiating system with a fixed component ratio of 1.5/3/0.2 wt % was used in each case. Although incorporating MsOH is highly beneficial in inducing predictable induction times in highly reactive mixtures, the less reactive aliphatic thiol TTT-SH monomer mixtures were easily handled and molded without any acid inclusion. Thereby, for the TTT-SH-based polymers an initiating system containing only TPP/DVS as the nucleophile and Michael acceptor at the ratio of 1/1 wt % was employed. Each monomer mixture also contained the photoinitiator IR 651 (DMPA, 1 wt %).

To assess the evolution of mechanical properties after the transition from the initial stage I polymer network to the ultimate, highly cross-linked stage II network polymers as well as the stage II methacrylate homopolymerization kinetics, three PETMP/HMDI/IEM compositions were prepared with varied cross-linking densities and methacrylate content at the end of the initial stage I reaction. The IEM monomer, which has both the isocyanate functionality and methacrylate functionality allows for the ability to tether the unreacted methacrylate functional groups within the initial polymer network. Therefore, the molar concentration of methacrylate functional groups can be varied with the IEM concentration within each formulation, and was increased from 1.33 M for composition number 1−2 M for the second composition to 2.66 M for the third, respectively. Proportionally, the HMDI molar concentration, which contains only the isocyanate functionality decreased in the same order from 3.33 to 3 to 2.66, respectively. The tetrathiol PETMP concentration remained constant at 2 M. An idealized typical cross-linked network after the initial stage I reaction is depicted in Figure 1, with the thiol-isocyanate reaction proceeding stoichiometrically to completion and leaving the residual unreacted methacrylate functional groups.

Typically, at the end of the initial thiol-isocyanate anionic polymerization reaction, a cross-linked polymer network in which the thiol functional groups and the isocyanate functional groups are fully consumed should be formed. To confirm the functional group conversions and characterize the resulting cross-linked polymer networks, we characterized all three formulations in terms of monomer conversion, glass transition temperature (T_g), and the extent of cross-linking.

The incorporation of a difunctional IEM reactant and the high selectivity in the reaction between thiols and isocyanates vs. methacrylates,[30,31] along with the ideal stoichiometry of the system allows for the first-stage thiol-isocyanate polymer formed to react completely while the methacrylate groups remain unreacted and pendent within the network. Kinetic data in the near-IR region for the stage I thiol-isocyanate step-growth network polymers leads to several conclusions. First, there is a proportional increase in absorbance of the methacrylate double bonds with increasing IEM content after the first stage reaction, indicative of their stability/inertness during the thiol-isocyanate reaction. Secondly, the thiourethane peaks do not change after thermal postcuring, which suggests complete conversion of all thiols and isocyanates originally present in the mixtures.

Additionally, similar thiourethane peaks for all three samples indicates complete stage I conversion because all tested samples had almost identical amount of thiol/isocyanate functional groups per sample volume. The near IR spectra after thiol-isocyanate step-growth reaction and thermal annealing at 60 °C for each of the three tested systems are included in Figure S1 in the Supporting Information.

From the materials property development standpoint, it is essential to evaluate the rate of methacrylate photopolymerization in glassy stage I polymers, especially if all methacrylate functionalities are fully tethered and their mobility is therefore significantly restricted. Figure 2a depicts methacrylate conversions vs. irradiation times for PETMP/HMDI/IEM compositions with varying IEM molar content. Generally, conversions after 20 min of continuous irradiation were low (between 25 and 40%) because the glassy nature of the networks imparts high restrictions in mobility of methacrylate functional groups. Predictably, the higher the concentration of

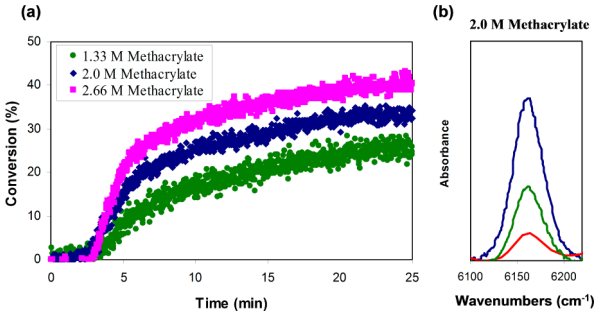

Figure 2. Near-IR kinetic data showing significant restrictions in (a) methacrylate conversion vs. irradiation time for PETMP/HMDI/IEM compositions with varying HMDI/IEM molar ratios: 3.33 M/1.33 M (green curve), 3.0 M/2.0 M (dark blue curve), 2.66 M/2.66 M (pink curve). PETMP concentration remains constant at 2 M. The irradiation intensity was set to 50 mW/cm^2. (b) Infrared signal for the methacrylate double bond in PETMP/HMDI/IEM for thermally annealed samples with 2 M IEM content: before irradiation (dark blue curve), after 15 min irradiation with 5 mW/cm^2 UV light at 100 °C (green curve), and after 15 min irradiation with 5 mW/cm^2 UV light at 100 °C and thermal annealing for 1 h at 150 °C (red curve).

reactive methacrylate sites, the higher the second-stage conversions as evidenced by double bond consumption rates increasing with increasing methacrylate (IEM) concentration. As the maximum conversions attained at ambient temperatures were seen to be relatively low, the reaction kinetics were also studied at elevated temperatures. In these kinetic experiments, samples containing no UV absorber were evaluated.

Figure 2b shows near IR signals of methacrylate groups for the intermediate composition cured for a varied amount of time at temperatures high above ambient. When the sample was irradiated for 15 min at 100 °C, the double bond conversions achieved were almost two times higher in spite of the UV light intensity reduction by 10 times. When the same sample was subsequently thermally annealed for 1 h at 150 °C, the conversion increased to more than 80%. Although long-term thermal postcure at high temperatures depleted the reactive sites considerably, quantitative conversions were not obtained, implying severe mobility restrictions within the polymer network, even at elevated temperatures. It is of interest to note that despite conducting the photopolymerizations at temperatures well above the glass-transition temperatures of the stage II polymers, the conversions were incomplete, as the tethered methacrylate groups were inaccessible for radical reaction.

The range of initial and final polymer properties as associated with the stage I thiol-isocyanate reaction and stage II photoinitiated methacrylate homopolymerization was evaluated in dynamic mechanical analysis (DMA). The importance of the extent of mechanical data shift in terms of modulus and T_g stems from the fact that these characteristics are the parameters that would define the material's response in any modulus gradient driven transformation. The DMA curves for fully or maximally cured polymer samples after each stage can be found in Figure S2 in the Supporting Information.

The versatility of the analyzed systems is attested to by simple variations in the HMDI/IEM ratio, which enables a judicious balancing between stage I and stage II properties. This behavior is manifested in a decrease of stage I T_g from 55 to 47 and 41 °C for compositions as the methacrylate content increases, and in an increase in stage II T_g values in the same order from 79 to 88 and 98 °C. An analogous trend can be seen in rubbery moduli values, which are proportional to the material's cross-linking density. On the basis of these properties, the first-stage cross-linking density decreases as the methacrylate content increases, whereas the second-stage cross-linking density increases with increasing methacrylate concentration. As evidenced by the tangent δ width at its half peak, the stage II networks are more heterogenous than the stage I networks, and the heterogeneity increases with increasing methacrylate content. On the basis of the first-, versus second-stage T_g difference, and the temperature under which the experiments were conducted, the intermediate methacrylate level was selected for most of the mechanically assisted 3D transformations as well as programming of topographical shapes. To assess the extent of the cross-linking density (modulus) gradient, polymeric films of PETMP:HMDI:IEM = 2M:3M:2M containing UV absorber (0.6 wt %) were exposed to UV light (5 mW/cm^2) on both sides for varying amounts of time, i.e., 1, 3, 4, 5, and 10 min. The film thickness was set to 0.25 mm by using appropriate spacers. The amount of UV absorber (T328) was calculated in such a way as to attenuate the light severely within an approximately 0.1 mm thick layer on both sides of the polymeric film, thus retaining a thin stage I (i.e., uncured methacrylate) middle layer. Samples fabricated according to this methodology were evaluated by dynamic mechanical examination. The DMA second heating curves are depicted in Figure 3.

From Figure 3a, it can be seen that the rubbery modulus is a function of irradiation dose, and increases with increasing dosage from 6 MPa for an unexposed sample to 15 MPa for the sample irradiated uniformly for 10 min on both sides. Even

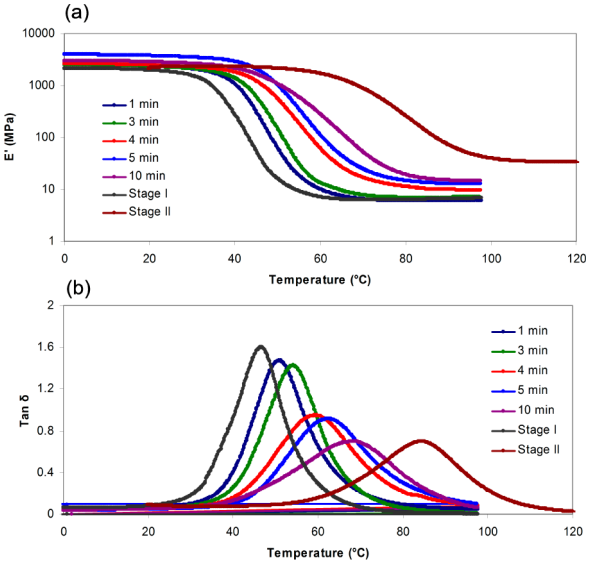

Figure 3. DMA results for absorber-containing samples (0.6 wt % T328) irradiated on both sides with 5 mW/cm^2 UV light for varying amounts of time (1−10 min). All samples were prepared from PETMP/HMDI/IEM at molar ratios of 2/3/2: (a) storage modulus vs. temperature curves and (b) tangent δ vs. temperature curves. Included are stage I and stage II DMA curves for neat bulk cured samples irradiated for 10 min with 5 mW/cm^2 with no UV absorber added. It can be seen that with increasing exposure time, the rubbery modulus and T_g gradually increase, although the presence of the absorber effectively prevents the material from achieving mechanical properties at a comparable level with fully cured stage II sample.

dx.doi.org/10.1021/am405371r | ACS Appl. Mater. Interfaces 2014, 6, 6111−6119

though the average cross-linking density doubles, this increase is still less than half of the cross-linking density that was attained in a maximally cured control sample in the absence of the UV absorber. Further, all absorber-containing samples exhibit significantly lower T_g values than fully cured stage II control samples, suggesting that there is no visible postcure involved (Figure 3b). The dramatic decrease in polymerization rates with increasing light absorption/attenuation amplified by restrictions associated with the limited mobility of pendent methacrylate groups are the primary reasons that enable the preservation of the stable property gradient. Another interesting observation indicative of the gradient is evidenced in the trend of increasing heterogeneity with exposure time. Despite the lower T_g, the sample exposed for 10 min appears to be more heterogenous than the much more cross-linked, fully cured stage II control sample. This behavior results from the cross-linking gradient that obviously increases the range of mobilities in the network, contributing greatly to the broadening of the relaxation times.

Temperature-Driven Stress Relaxation and Associated Geometry Changes in Strained Glassy Films with Depth-Wise Cross-linking Gradients. Here, we demonstrate that localized stress relaxation in gradient property polymers, controlled by simultaneous but independent variation of the strain extent and temperature, result in 3D materials reshaping as well as creation of topographical surface features. Moreover, the advantageous mechanical properties of the two-stage networks are beneficial in designing new materials for advanced technologies, and represent an exciting addition to currently known processing techniques.

For the sake of discussion, the gradient property material can be treated as a laminate, made of multiple layers of variable cross-linking density. Stretching such a material requires uniform straining of all the layers. The stress build-up associated with the uniform strain, however, will be lower in layers with lower cross-linking density as the force required to strain each underlying layer by the same length will be decreased with the lowered modulus associated with the lower cross-link density. Once the strain is released at an elevated temperature that is above the T_g of the layers, every one of the strained layers will tend to spring back to their original shape. This rate of shape recovery will differ in layers - with the surface, highly cross-linked layers recovering their shape at the fastest rate. Now, if we instead introduce a cooling of the thin laminate-like structure to an intermediate temperature below the T_g of some of the layers and above that of others, some of the layers will not regain their shape in full due to vitrification. Once the whole laminate is heated above its T_g, all of its layers will regain their original shape, unless reacted further (Figure 4).

Therefore, the difference in the rate of strain relaxation in an uniaxially strained material with a depth-wise cross-linking density gradient at a given temperature causes it to deform in the direction dictated by the gradient, whereas new shape preservation/programming can occur because of the difference in vitrification and cross-linking densities. Photoirradiating through appropriately designed photomasks enables the property gradients to be readily created in predefined regions of the glassy materials, which can then be used to form samples of the desired geometries.

Initially, to evaluate the extent of material deformation possible and this overall approach, we irradiated stripe-shaped samples for a fixed amount of time on both sides with a 2.5 mm

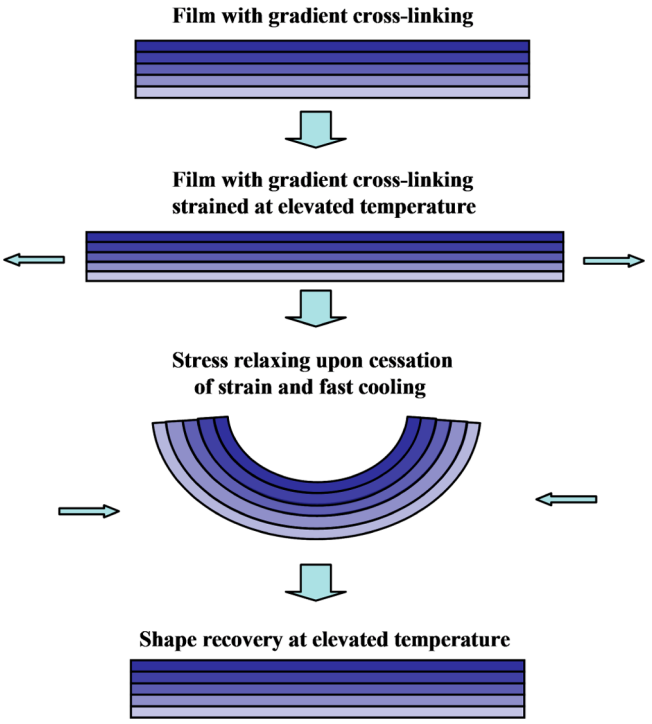

Figure 4. Temperature-driven stress relaxation and associated geometry changes in a laminate with gradient cross-linking (dark blue, highly cross-linked layer; light blue, lowly cross-linked layer) and without any additional reaction during the heating/straining/cooling cycle. The ability to modulate inherent stresses by strain and cooling rate is used to form functional geometric objects or patterns.

screening band attached on one side preventing the light from coming through as shown in the inset of Figure 5. Thus, for these experiments, illumination was prevented in only a single narrow band on one side of the sample to leave a uniform modulus film in the unexposed sample at that surface. Subsequent straining of the sample at 40 °C was used to cause the desired bending to occur, because of differential relaxation in the unexposed region.

Specifically, after UV irradiation (5 mW/cm^2), the samples were mechanically stretched by 15 % at 40 °C, and then the buildup in stress was relaxed upon releasing the strain while cooling the samples at ambient temperature. The specimen deformation range was evaluated as a change in the bending angles plotted against irradiation times that are proportional to the degree of the gradient in cross-linking. During photo-irradiation of absorber-containing films, polymerization proceeds deeper and deeper into the irradiated material with continued exposure times.[23,27] However, because of a lack of bleaching here, as was indicated before (Figure 2), continuous exposure to UV light for a longer time does not lead to quantitative conversion of double bonds, which implies that the property gradient will not be compromised even after long exposure times. Additional proof can be found in visibly affected homogeneity of the networks with distinct and deep modulus gradient (Figure 3). Therefore, the control over gradient programming appears to be facilitated in glassy polymers where the second-stage reaction is significantly restricted by the immobile matrix. As can be seen from Figure 5, bending angles, and by extension, shape programming, can be finely adjusted by the light dose, here extending from 1 to 10 min irradiation. The material's response is also tuned by

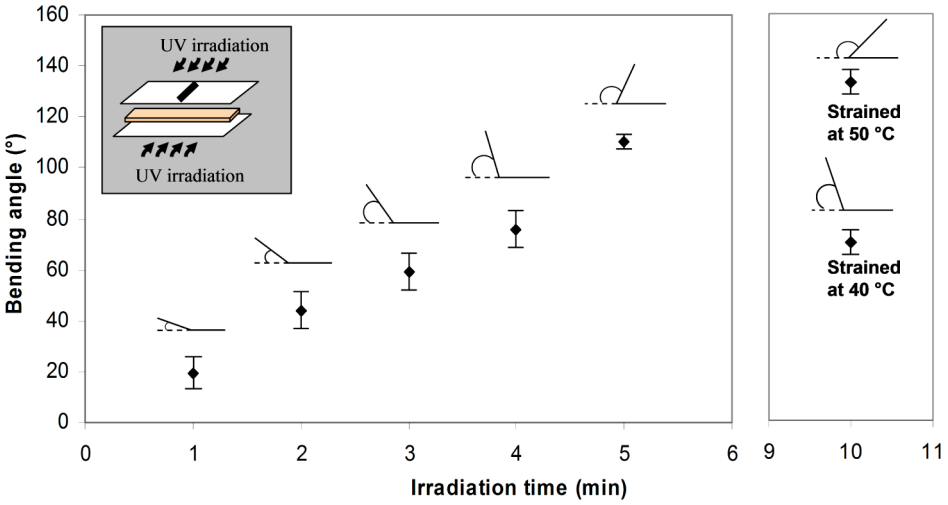

Figure 5. Tinuvin-containing sample bending angles versus irradiation times for PETMP/HMDI/IEM systems composed at molar ratios of 2/3/2, and irradiated with 5 mW/cm^2 UV light from 1 to 10 min, then stretched by 15% at 40 °C, and relaxed at ambient. Inset depicts the irradiation setup. The extent in directional sample deformation increases with exposure times and/or relaxation temperature. Actual sample images can also be found in Figure S3 in the Supporting Information.

changing the temperature of relaxation, allowing for different geometries from identically photocured specimens as evidenced by two drastically different bending angles achieved by straining the sample exposed for 10 min at 40 and 50 °C, respectively (Figure 5). To demonstrate the effectiveness of this methodology, multiple 3D geometries were conveniently prepared as illustrated in Figure 6. Shapes such as ribbons, lenses, boxes, and others were fabricated from appropriately adapted stage I polymeric films strained after irradiation in uniaxial, biaxial, or radial modes. The second-stage curing time varied from 90 to 180 s, whereas the samples strain spanned the range of 15–25%. The temperature of the strain relaxation was set to 40 °C.

In preparing the shapes described above, the thiourethane first-stage networks were strained up to 25% after the second-stage gradient reaction. As mentioned previously, the average rubbery moduli of these networks are much less than 15 MPa, which implies quite low cross-linking density, e.g., 7 MPa in the sample irradiated for 3 min. Therefore, the generated property gradient does not contribute much to the bulk modulus and T_g values of the unexposed material, which are 41 °C and 6 MPa, respectively. In other words, the bulk properties of the property gradient materials are defined mostly by the stage I network features, assuming relatively short curing times, i.e., shorter than 3 min for stage II (see DMA results in Figure 3). The predominance of stage I properties is highly beneficial because the thiourethane step-growth networks are known to be uniform, elastic, and tough polymers.[31] There are a considerable amount of thiourethane linkages in them that are quite rigid and capable of hydrogen bonding. On the other hand, the flexible PETMP-derived cross-links are expected to contribute positively to the materials' elasticity. Therefore, these intricate-gradient thiourethane networks can be strained by much more than 25%. Indeed, the following profilometry data has been collected on photopatterned films strained by as much as 45% without any material failure. The rectangular-shaped stage I films were photopatterned through three different masks and the periodic line patterns were then achieved by straining by 20, 40 (or 45 %). Stylus profilometry runs were performed in those strained configurations (Figure 7).

Because the experiments were done at ambient temperature, there was no relaxation observed in the samples during or after the data collection. As can be seen from Figure 7, a facile fabrication of complex topographical features of varying depths can be easily achieved by controlling the strain and proper mask selection. It should also be noted that the strain-induced topographic features can be erased on demand once the polymer is exposed to elevated temperatures. Interestingly, after heating of the patterned polymeric films without straining, faint surface profiles can be discerned (unstrained samples in Figure 7b, c), which suggests that by tuning the gradient property range, three-dimensional objects can be triggered to form by heating. This outcome seems plausible because methacrylate gradient homopolymerization is likely to generate significant gradients in shrinkage stress, which when partially relieved at elevated temperatures, still constitute a sufficient driving force for material geometry changes. Additionally, it would be very beneficial if the once created and desired surface features or 3D shapes were locked in their shape permanently and on demand. To attain this feature, a dramatic increase in modulus/cross-linking is required and an improved two-stage system is needed. To create such a system, a trifunctional aliphatic thiol (TTT-SH) having in its core a rigid triazine-trione derived ring was synthesized and used for stage I polymer fabrication. The compositions of the reactants were fixed to assure a loosely cross-linked stage I material (TTT-SH:HMDI:IEM = 1M:1M:1M). In an ideally nonselective reaction where every IEM molecule is attached to one thiol group, a linear system should be formed as shown in Figure S4 in the Supporting Information. Here, a loosely cross-linked network polymer was obtained with a theoretical gel point conversion of 86% (according to Flory–Stockmayer equation) and a rubbery modulus lower than 1 MPa (see Figure S5 in the Supporting Information).

Despite the relatively low cross-link density, the polymer T_g was found to be well beyond ambient (65 °C). After a stage II flood-cure of the pendant methacrylate functionalities, a significant increase in the modulus (up to 22 MPa) and T_g (above 125 °C) was observed (DMA data in Figure S5 in the Supporting Information).

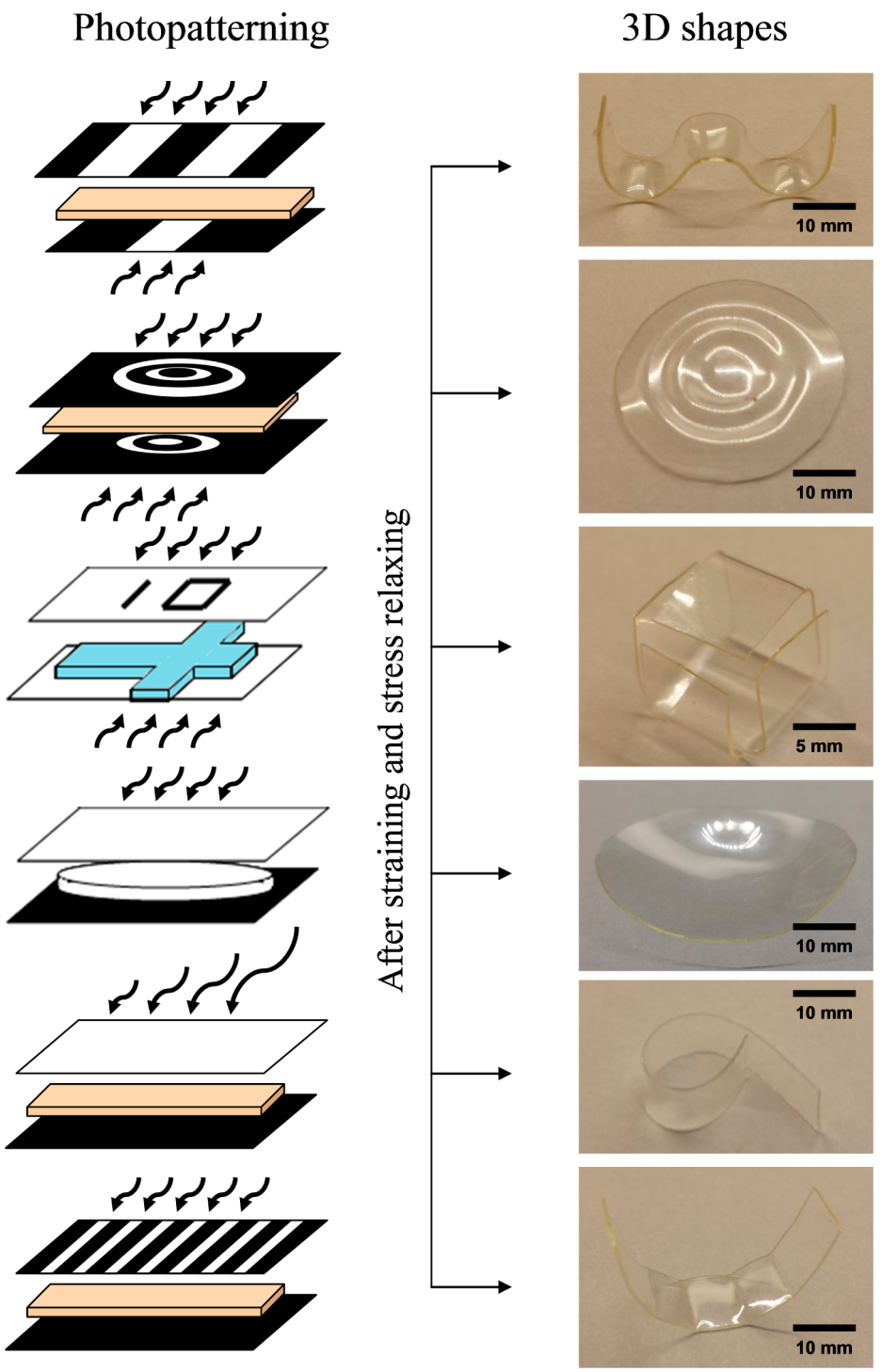

Figure 6. General methodology of achieving different geometric object by exposing samples of predefined shapes through appropriately designed photomasks. The programmed configurations were invoked by uniaxial, biaxial or radial straining followed by strain relief at elevated temperatures (40 °C). For specific 3D objects, the exposure time varied from 90 to 180 s, whereas the samples strain spanned the range from 15 to 25%.

Into a similar system, two photoortoghonal initiators, i.e., IR 651 and IR 819 that are capable of initiating at two different wavelengths, were incorporated together with a UV absorber (T328). Both photoinitiators can be cleaved by 365 nm light source to create a desired gradient, whereas a relatively uniform bulk polymerization is initiated by IR819, which also absorbs in the visible spectral range above 400 nm. A stripe-shaped film was irradiated on both sides through a positive mask on one side and negative on the other just as shown in Figure 8.

After irradiation, the film was heated at 80 °C to reveal a patterned shape (2). Straining by 15% and consecutive relaxing resulted in even more distinct features (3). Uniform flood-curing by visible light, whereas heating of shape (2) resulted in a new permanent shape (4). As anticipated, a significant cross-linking density gradient allowed for these shape changes without straining, whereas significant increase in bulk cross-linking density after stage II enabled shape fixation.

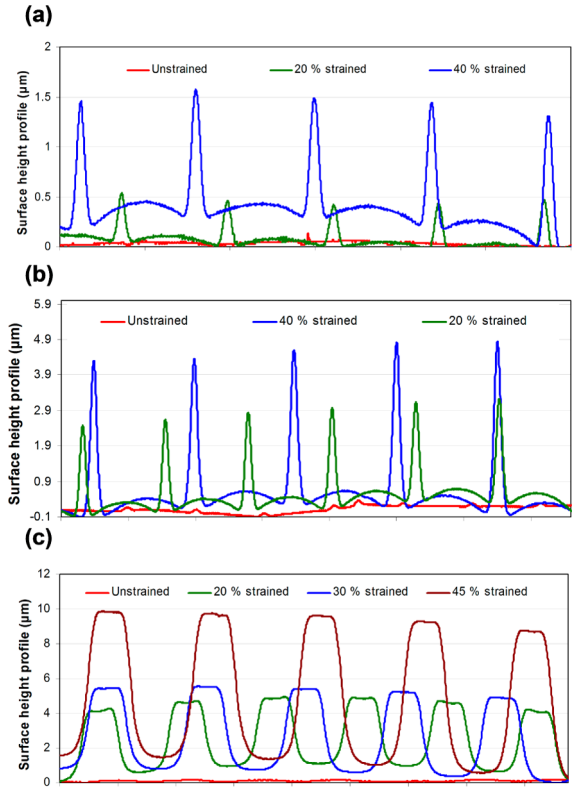

Figure 7. Stylus profilometry of surface height features for PETMP/HMDI/IEM rectangular samples made at molar ratios of 2/3/2 and irradiated through three photomasks with micrometer-size strips: (a) 5/500, (b) 10/500, and (c) 100/150. The profilometry runs were performed on samples held in strained configurations with the strain spanning 20–45% as indicated in the figure. Irradiation intensity was set to 50 mW/cm^2 and the exposure was carried out on one side for 90 s.

CONCLUSIONS

The versatility of two-stage reactive polymers in generating material geometry changes in either bulk macroscopic deformations or in elaborate topographical patterns, such as mechanical instabilities that can reappear or disappear under the influence of an external stimulus has been demonstrated. These elastic instabilities are easily induced in bulk as well as in predefined, patterned regions of the two-stage reactive systems. Hence, these materials have the potential for creating materials with the possibility of modulating macroscopic shape, microscopic topography, and patterned material properties within those geometries. By introducing thiourethanes and methacrylate homopolymerization in the networks, we designed systems in which the property gradients are tunable to enable fabrication of geometric objects of the desired shape and function. This methodology utilizes tough glassy materials, which exist after each of the polymerization steps. These materials hold their shape in strained configurations, which enables shape programming followed by shape fixation of the new geometries. Further, intricate surface features can be programmed and "locked" on demand. In addition, introducing gradients of properties in glassy systems can be used to create "hidden" patterns that are visualized only upon straining/heating. As a whole, new shape memory transformations were demonstrated with the possibility of temporal/permanent shape switching and associated property changes.

ASSOCIATED CONTENT

Supporting Information

Experimental kinetic profiles, DMA plots, and monomer characterization data. This material is available free of charge via the Internet at http://pubs.acs.org.

AUTHOR INFORMATION

Corresponding Author

*E-mail: christopher.bowman@colorado.edu.

Notes

The authors declare no competing financial interest.

ACKNOWLEDGMENTS

The authors acknowledge the National Science Foundation DMR 1310528 for providing funding for this research.

REFERENCES

(1) Chan, E. P.; Crosby, A. J. *Adv. Mater.* **2006**, *18*, 3238–3242.
(2) Chan, E. P.; Smith, E. J.; Hayward, R. C.; Crosby, A. J. *Adv. Mater.* **2008**, *20*, 711–716.
(3) Zhao, Q.; Behl, M.; Lendlein, A. *Soft Matter* **2013**, *9*, 1744–1755.

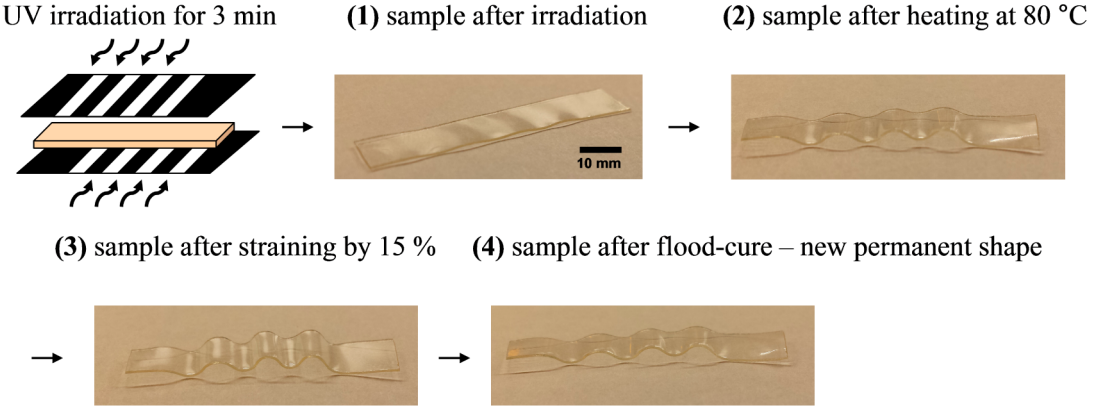

Figure 8. Shape change/fixation by heating/straining a patterned stage I network. Composition tested: TTT-SH/HMDI/IEM = 1M/1M/1M. Sample thickness, 0.25 mm; UV absorber content, 0.6 wt %; photoinitiator IR 651 concentration, 1 wt %; photoinitiator IR 819 concentration, 1 wt %; irradiation intensity, 5 mW/cm^2. (1) Sample shape after 3 min irradiation; (2) shape change of irradiated sample at 80 °C; (3) shape change of irradiated and 15 % strained sample at 80 °C; (4) shape fixation with associated modulus increase by uniform flood-cure of residual methacrylate functionalities by visible light irradiation (50 mW/cm^2).

(4) Bowden, N.; Brittain, S.; Evans, A. G.; Hutchinson, J. W.; Whitesides, G. M. *Nature* **1998**, *393*, 146−149.
(5) Stafford, C. M.; Harrison, C.; Beers, K. L.; Karim, A.; Amis, E. J.; Vanlandingham, M. R.; Kim, H. C.; Volksen, W.; Miller, R. D.; Simonyi, E. E. *Nat. Mater.* **2004**, *3*, 545−550.
(6) Lendlein, A.; Kelch, S. *Angew. Chem., Int. Ed.* **2002**, *41*, 2034−2057.
(7) Zhang, D. Y.; Jiang, H. Q.; Huang, Y.; Rogers, J. A. *Science* **2006**, *311*, 208−212.
(8) Duerig, T. W.; Stoeckel, D.; Pelton, A. *Mater. Sci. Eng.* **1999**, *273*, 149−160.
(9) Nair, D. P.; Cramer, N. B.; Gaipa, J. C.; McBride, M. K.; Matherly, E. M.; McLeod, R. R.; Shandas, R.; Bowman, C. N. *Adv. Funct. Mater.* **2012**, *22*, 1502−1510.
(10) Agarwal, P.; Chopra, M.; Archer, L. A. *Angew. Chem., Int. Ed.* **2011**, *50*, 8670−8673.
(11) Miaudet, P.; Derre, A.; Maugey, M.; Zakri, C.; Piccione, P. M.; Inoubli, R.; Poulin, P. *Science* **2007**, *318*, 1294−1296.
(12) Defize, T.; Riva, R.; Jérôme, C.; Alexandre, M. *Macromol. Chem. Phys.* **2012**, *213*, 187−197.
(13) Leng, J.; Lan, X.; Liu, Y.; Du, S. *Prog. Mater. Sci.* **2011**, *56*, 1077−1135.
(14) Behl, M.; Razzaq, M. Y.; Lendlein, A. *Adv. Mater.* **2010**, *22*, 3388−3410.
(15) Hu, Y.; Chen, W. *Macromol. Chem. Phys.* **2011**, *212*, 992−998.
(16) Nair, D. P.; Cramer, N. B.; Scott, T. F.; Bowman, C. N.; Shandas, R. *Polymer* **2010**, *51*, 4383−4389.
(17) Mather, P. T.; Luo, X. F.; Rousseau, I. A. *Annu. Rev. Mater. Res.* **2009**, *39*, 445−471.
(18) Efimenko, K.; Finlay, J.; Callow, M. E.; Callow, J. A.; Genzer, J. *ACS Appl. Mater. Interfaces* **2009**, *1*, 1031−1040.
(19) Schumacher, J. F.; Carman, M. L.; Estes, T. G.; Feinberg, A. W.; Wilson, L. H.; Callow, M. E.; Callow, J. A.; Finlay, J. A.; Brennan, A. B. *Biofouling* **2007**, *23*, 55−62.
(20) Davis, C. S.; Martina, D.; Creton, C.; Lindner, A.; Crosby, A. J. *Langmuir* **2012**, *28*, 14899−14908.
(21) Chandra, D.; Yang, S.; Lin, P. C. *Appl. Phys. Lett.* **2007**, *91*, 251912.
(22) Yang, S.; Khare, K.; Lin, P. C. *Adv. Funct. Mater.* **2010**, *20*, 2550−2564.
(23) Kim, H. S.; Crosby, A. J. *Adv. Mater.* **2011**, *23*, 4188−4192.
(24) Chung, J. Y.; Chastek, T. Q.; Fasolka, J. M.; Ro, H. W.; Stafford, C. M. *ACS Nano* **2009**, *3*, 844−852.
(25) Kloxin, C. J.; Scott, T. F.; Park, H. Y.; Bowman, C. N. *Adv. Mater.* **2011**, *23*, 1977−1981.
(26) Nair, D. P.; Cramer, N. B.; McBride, M. K.; Gaipa, J. C.; Lee, N. C.; Shandas, R.; Bowman, C. N. *Macromol. Symp.* **2013**, *329*, 101−107.
(27) Ma, S. J.; Mannino, S. J.; Wagner, N. J.; Kloxin, C. J. *ACS Macro Lett.* **2013**, *2*, 474−477.
(28) Lundberg, P.; Bruin, A.; Klijnstra, J. W.; Nystrom, A. M.; Johansson, M.; Malkoch, M.; Hult, A. *ACS Appl. Mater. Interfaces* **2010**, *3*, 903−912.
(29) Chatani, S.; Sheridan, R. J.; Podgórski, M.; Nair, D. P.; Bowman, C. N. *Chem. Mater.* **2013**, *25*, 3897−3901.
(30) Hensarling, R. M.; Rahane, S. B.; LeBlanc, A. P.; Sparks, B. J.; White, E. M.; Locklin, J.; Patton, D. L. *Polym. Chem.* **2011**, *2*, 88−90.
(31) Matsushima, H.; Shin, J.; Bowman, C. N.; Hoyle, C. E. *J. Polym. Sci., Part A: Polym. Chem.* **2010**, *48*, 3255−3264.